

Controlling the Morphology of Polyurethane/Polystyrene Interpenetrating Polymer Networks for Enhanced Blood Compatibility

J. H. KIM, S. C. KIM

Center for Advanced Functional Polymers, Korea Advanced Institute of Science and Technology, 373-1, Kusong-dong, Yusong-gu, Taejeon 305-701, Korea

Received 20 October 2000; accepted 11 June 2001

ABSTRACT: Polyurethane (PU)/polystyrene (PS) IPNs were simultaneously synthesized at 80°C, controlling the reaction kinetics to change the morphology. Polymerization kinetics of styrene was controlled by the content of initiator, and that of polyurethane by the catalyst concentration. The effect of the initiator and the catalyst on the polymerization rate was analyzed by NMR spectroscopy and FTIR. Gelation time was also measured by using the advanced rheometric expansion system (ARES). Samples with sea-and-island morphology were obtained, when the polymerization rate of PS was relatively slow, and the phase separation time was long. When the polymerization rate of PS was relatively fast, and the phase separation time was short, cocontinuous morphology was obtained. The degree of phase separation and surface roughness decreased, as the rate of PU network formation was increased, and the phase-continuity was increased. The *in vitro* blood-compatibility tests showed that the surface roughness was an important factor on the adsorption of fibrinogens and platelets. A large amount of fibrinogens and platelets were adsorbed on the relatively rough surface of samples showing sea-island morphology. © 2002 John Wiley & Sons, Inc. *J Appl Polym Sci* 84: 379–387, 2002; DOI 10.1002/app.10358

Key words: IPNs; phase separation; morphology; biocompatibility

INTRODUCTION

Biocompatibility, especially blood compatibility, is influenced by the surface properties of the materials, such as morphology, roughness, hydrophilicity, etc. Surface morphology of the multicomponent polymers shows different types of morphology, sea-island, cocontinuous, and dual-phase coexistence of sea-island and cocontinuous morphology, due to different mechanisms of phase separation. The morphology can be changed by the kinetic and/or thermodynamic fac-

tors.^{1–8} Nucleation and growth is the dominating phase separation mechanism in the metastable region of the phase diagram. In this region, when a nucleus is formed, it grows by a normal diffusion process, and sea-and-island morphology is developed. Spinodal decomposition occurs in the unstable region. In the unstable region, the concentration fluctuations are delocalized and the phase separation takes place spontaneously, leading to long-range phase segregation. In this mechanism, cocontinuous morphology is developed when the separation is stopped at an early stage. In the reaction-induced phase separation, the relative rate of polymerization to the rate of phase separation is an important factor to determine the degree of phase separation, and the relative

Correspondence to: S. C. Kim.

Journal of Applied Polymer Science, Vol. 84, 379–387 (2002)
© 2002 John Wiley & Sons, Inc.

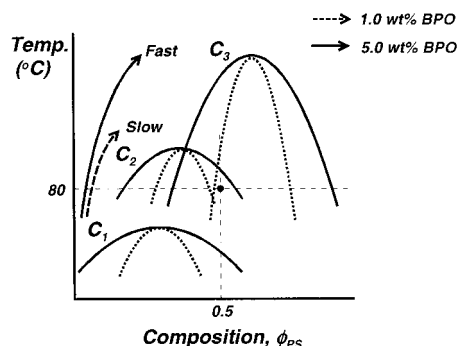


Figure 1 Schematic phase diagram of simultaneously polymerized PU/PS IPNs.

rate of polymerization of each component also influences the phase separation mechanism. The degree of phase separation and the morphology affect the surface properties, such as the surface roughness, hydrophilicity, elasticity, and hardness. Particularly, the surface roughness affects the adsorption of proteins, and platelets. The initial protein adsorption, and cell attachment on a surface is increased, as the surface roughness is increased, and this effect is related to the size of proteins and cells adhered.^{9–13}

In 1994, S. C. Kim and his coworkers reported that hydrophilic PU/hydrophobic PS IPNs exhibited good blood compatibility as well as excellent mechanical properties. They also investigated the effect of the degree of phase separation on blood compatibility with controlled morphology.^{14–16} The reaction temperature, composition of monomers, and crosslink density considerably affected blood compatibility because the size of the dispersed PS domain was affected by those conditions. As a result, protein adsorption and platelet adhesion decreased as the size of the PS domains decreased. Recently, they grafted PEO chains to a PU network of PU/PS IPNs to suppress protein adsorption and platelet adhesion. As a result, they observed enhanced blood compatibility of the PU/PS IPNs.¹⁷

In this study, polyurethane (PU)/polystyrene (PS) interpenetrating polymer networks (IPNs) were synthesized simultaneously, controlling the kinetic conditions to change the morphology, and the degree of phase separation. Polymerization kinetics of styrene was controlled by the content of an initiator, and that of polyurethane was done by the catalyst concentration. Figure 1 shows the scope of this study. In this schematic phase diagram, the immiscible region increases with increasing the PS conversion, and this trend be-

comes much faster as the polymerization rate of styrene is increased. The phase separation during the synthesis of PU/PS IPN with low content of BPO, the initiator, may start in a meta-stable region, and the phase diagram at low PS conversion becomes a dominant diagram to determine the final morphology of PU/PS IPN. As a result, the final morphology of PU/PS IPN shows sea-and-island. However, in the synthesis of PU/PS IPN with high content of BPO, the immiscible region is rapidly increased, and the phase diagram to determine the morphology may be that at the higher PS conversion. As a result, PU/PS IPN has the final morphology of a cocontinuous type. Various types of morphology cause the change of surface properties, as previously stated. This change considerably affects blood compatibility, and the effect is investigated in this study.

EXPERIMENTAL

Materials

Poly(ethylene glycol) (PEG, $M_w = 600$, Junsei Chemical Co., Ltd.), 1,4-butanediol (1,4-BD, Junsei Chemical Co., Ltd.) and trimethylolpropane (TMP, Acros Organics) for the PU network were degassed for 12 h under vacuum to remove moisture before use. Styrene monomer (SM, Showa Chemical Co., Ltd.) was purified by the conventional method.¹⁸ Hexamethylene diisocyanate (HDI, Tokyo Kasei Kogyo Co., Ltd.), divinylbenzene (DVB, Aldrich Chemical Company, Inc.) as a crosslinking agent for PS network, and benzoyl peroxide (BPO, Fluka Chemika) as an initiator for the polymerization of styrene were used without further purification.

Synthesis

The diisocyanate-terminated PU prepolymer (Fig. 2) was prepared by reacting 1 equiv. of poly(ethylene glycol) (PEG, $M_w = 600$) with 2 equiv. of HDI at 65°C for 2 h under N_2 atmosphere; 0.05 wt % dibutyltin-diaurate (T-12) as a catalyst was added to poly(ethylene glycol) before reaction. HDI was poured into a four-neck flask held at 65°C in a heating mantle, and the degassed poly(ethylene glycol) was added dropwise to HDI through a dropping funnel with vigorous stirring of the mixture. The completeness of the reaction was identified by the di-n-butylamine titration method,¹⁹ and the product was kept below 0°C

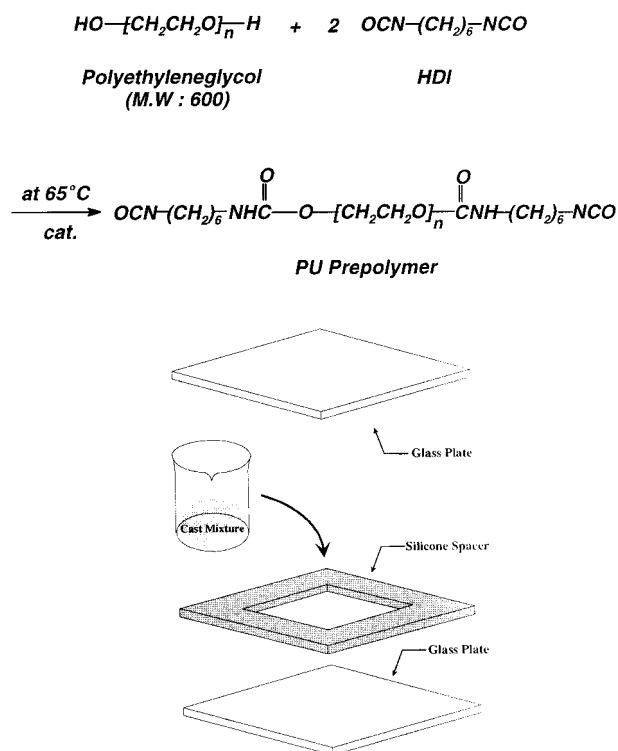


Figure 2 Synthetic scheme of PU prepolymer, and schematic diagram of cast mold.

after N_2 purging. The molecular structure of PU prepolymer was investigated by NMR spectroscopy.

PU/PS IPNs having various morphology were prepared by changing the reaction kinetics by varying the catalyst/initiator concentration. PU prepolymer, 1,4-BD, TMP, T-12, SM, DVB, and benzoyl peroxide were mixed by a high-torque stirrer in a 250-mL beaker for about 5 min. The mixture was degassed under vacuum for about 3 min, and then cast in a glass plate mold with a silicon spacer (Fig. 2). The PU network and PS network were formed simultaneously in a convection oven at 80°C for 10 h, and the postcuring was followed at 120°C for 2 h.

Kinetics

Conversion of styrene during the formation of PS network was measured with different initiator concentration (1.0 wt % to 5.0 wt % BPO) by using ^1H -NMR spectroscopy. During the polymerization, sample was taken in every 5 min, and dissolved in deuterated benzene for ^1H -NMR spectroscopy. The conversion was determined by analyzing the peak area of vinyl group portion of

styrene ($\text{CH}_2=\text{CHPh}$; $\delta 5.1$ – $\delta 5.8$ ppm, and $-\text{CH}_2-\text{CHPh}-$; $\delta 1.9$ – $\delta 2.3$ ppm). Conversion of isocyanate group during the formation of PU network with different catalyst concentration (0–0.05 wt % T-12) was measured by using FTIR equipped with demountable liquid cell, and heating accessory. The conversion was determined by observing the decrease of isocyanate peak area at 2271 cm^{-1} , caused by the formation of urethane linkage.

Gelation Time

Gelation conversion and time during PS synthesis, and PU synthesis were investigated by using ARES, and PHYSICA, respectively. Gelation time was determined by analyzing the shear modulus–time graph. At gelation time, G' , shear storage modulus increased and crossed the G'' , shear loss modulus curve, and the gelation conversion was calculated by using the kinetic data, previously obtained.

Morphology

The morphology of the top surface of the PU/PS IPNs was investigated by the scanning probe microscopy (SPM, DI NanoScope IIIa). SPM measurement was performed in air with an etched silicon probe, of which the length was $125\ \mu\text{m}$, and the spring constant was from 20 to $100\ \text{N/m}$. Scanning was carried out in the TappingTM mode, and its frequency was about 0.5 Hz.

Surface roughness was investigated by analyzing the three-dimensional SPM images with image analyzer.

Swelling Behavior in Water

PU homopolymer, and PU/PS IPN samples were dried at room temperature for 24 h under vacuum, and then immersed in distilled water until equilibrated with water. The weight of the sample was measured in every 15 min, and the swelling ratio was calculated by the following equation.

Interfacial Energy

Interfacial energy between water and the PU/PS IPNs, PU homopolymer surface was measured by the underwater captive bubble technique.²⁰ The samples were equilibrated with distilled water for more than 24 h, and the static bubble contact angles of the surface–water–air and the surface–water–octane were measured by a contact angle

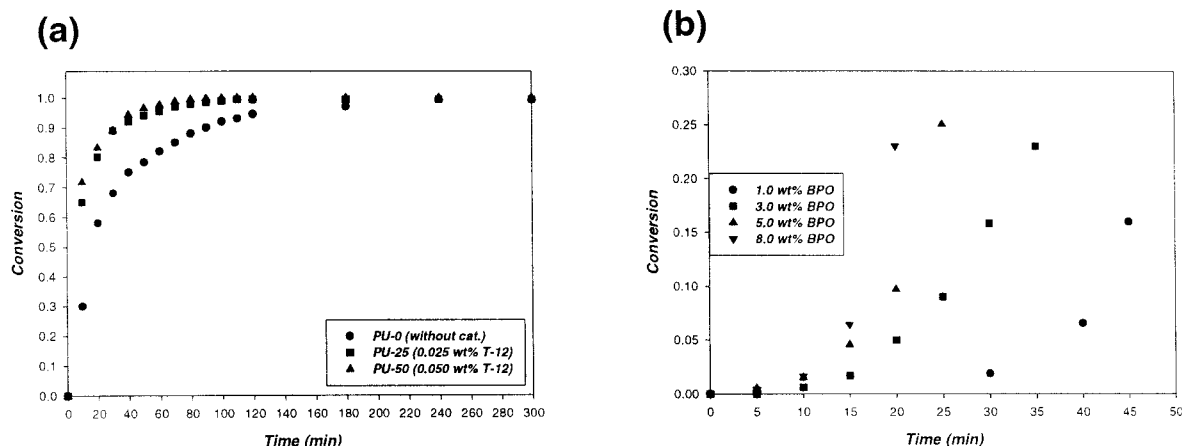


Figure 3 Kinetics of the polymerization: (a) polyurethane synthesis; (b) polystyrene synthesis.

goniometer (Erma model G-I type) equipped with an oil droplet apparatus in the water. Interfacial energy between the surface and the water was calculated from the geometric mean equation.

Fibrinogen Adsorption²¹

Fibrinogen is one of the most important globular proteins circulating in the blood. It plays a central role in the regulation of hemostasis and thrombosis by participating in blood coagulation and facilitating adhesion and aggregation of platelets. The BPF (ICN Biomedicals, Inc.) was dissolved in phosphate buffer saline (PBS) in a concentration of 30 mg/mL. Samples (5 × 1 × 20 mm) were immersed in the solution at 37°C under a mild shaking condition. To consider the adsorption of BPF's on the wall of the vial, a blank test was performed. After a series of immersion time (10, 20, 40, and 60 min), samples were removed, and the changes of the concentration in the solution were investigated by using an UV-spectrophotometer.

Platelet Adhesion²²

The adhesion and activation of the platelets on the surfaces of PU homopolymers and PU/PS IPNs were observed. After samples (10 × 10 mm²) were equilibrated with PBS overnight, they were then immersed in platelet-rich plasma (PRP), which was obtained from Taejon Red Cross, at 37°C with mild shaking in an incubator. After 10 h, the samples were taken out from the solution and rinsed five times with PBS to remove the weakly adsorbed platelets. Then the strongly ad-

sorbed platelets were fixed on the surfaces by immersing the sample in 2-v/v% glutaraldehyde PBS solution at room temperature for 2 h. After the fixation, the samples were dehydrated with a series of ethanol solutions (50, 60, 70, 80, 90, and 100 v/v%) for 15 min per each step. Then they were dried in atmosphere overnight and under vacuum for 5 h. The dried samples were coated with evaporated gold, and the adherent platelets were observed with Philips 535M SEM.

RESULTS AND DISCUSSION

Kinetics

Figure 3(a) and (b) shows the kinetics of PU synthesis and PS synthesis, respectively. The polymerization rate of styrene could only be measured before gelation, because the PS network could not be dissolved in NMR solvent after gelation. The reaction rate of isocyanate group in the PU synthesis increased as the content of the T-12 catalyst was increased from 0 to 0.05 wt/wt %. The polymerization rate of styrene increased as the content of BPO, the initiator, was increased from 1.0 to 8.0 wt/wt %, because the amount of free radicals, initially produced, was increased, and the initial polymerization rate also increased.

Gelation Time and Conversion

Figure 4 shows the change of G' , and G'' values during synthesis of PU and PS. In the synthesis of PU with 0.025 wt/wt % T-12, G' increased, and crossed the G'' -curve at 5.2 min, which means

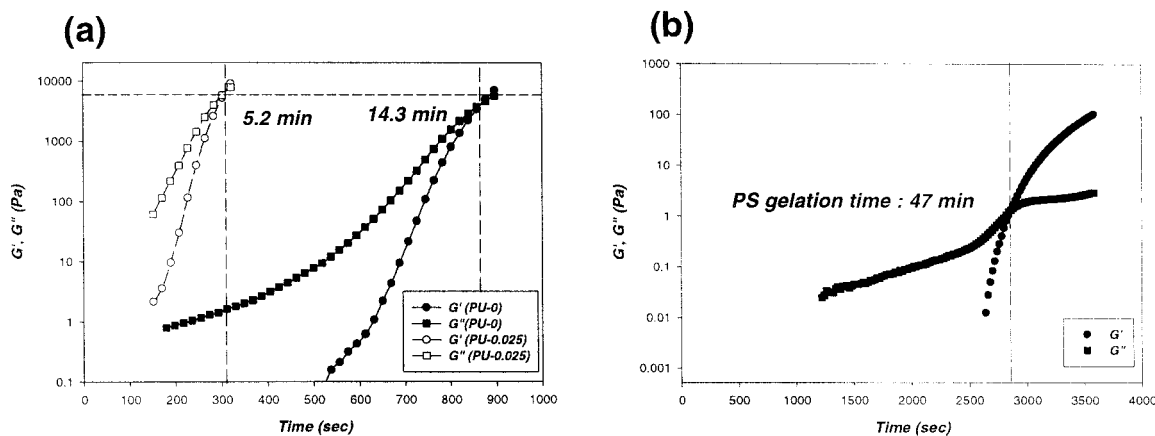


Figure 4 The change of G' , and G'' during the polymerization: (a) PU, \circ , \square ; with 0.025 wt % T-12, \bullet , \blacksquare ; without T-12; (b) PS with 1.0 wt % of BPO.

that the gelation occurred. In the synthesis of PU without a catalyst, gelation was delayed about 14.3 min. However, the gelation conversions in both cases were identical with each other at 0.55. In the synthesis of PS with 1.0 wt/wt % of BPO, gelation occurred at 47 min, and the gelation conversion calculated was 0.24. The gelation time with high BPO concentration was shown in Table I. The gelation time of PS network decreased from 47 to 24 min, as the content of BPO was increased from 1.0 wt/wt % to 5.0 wt/wt %.

Surface Morphology

Various surface morphology was observed, as the catalyst and initiator concentration was varied. The surface of PU/PS IPN synthesized with 0.025 wt/wt % of T-12, and 1.0 wt/wt % of BPO shows sea-island morphology. The PU-rich phase formed the continuous matrix, and the PS-rich phase formed the dispersed island. The surface of PU/PS IPN synthesized with 0.05 wt/wt % of T-12, and 1.0 wt/wt % of BPO also shows sea-island morphology, but the size of the dispersed PS-rich domains was much smaller, because the

Table I Gelation Time of PS Networks with Various Amounts of BPO

Content of BPO Involved (wt/wt %)	Gelation Time (min)
1.0	47
3.0	35
5.0	24

PU reaction was much faster, the gelation of PU occurred earlier, and the rate of phase separation was decreased, with the time of phase separation unchanged. During the synthesis of PU/PS IPNs with 1.0 wt/wt % of BPO PU reacted faster than PS, and the critical composition at the time of phase separation, $\phi_{s,c}$ became smaller than 0.5 (Fig. 1, C_1). The mixture composition 0.5 would enter the metastable region, as the reaction procedure and the dominant phase-separation mechanism would be nucleation and growth. However, when the BPO concentration was increased to 5.0 wt/wt %, the reaction rate of styrene became much faster, and the phase separation occurred at relatively lower conversion of PU, compared to the previous case, which means that the critical composition at the time of phase separation, ϕ_s became closer to 0.5 and the mixture composition 0.5 would enter the unstable region, as the reaction procedure and the dominating phase separation mechanism would be spinodal decomposition, which would give cocontinuous morphology. In the intermediate case with 3.0 wt/wt % BPO, both phase separation mechanisms could occur. Initially, the mixture composition, $\phi_s = 0.5$ would enter into the metastable region at the start of the phase separation but would enter the unstable region as the reaction proceeds, and the both sea-island and cocontinuous morphology was observed in this case. The morphological patterns were summarized according to the content of T-12, and BPO in Table II. The SPM images of surface morphology of the sample were shown in Figure 5. Surface roughness was also investigated by analyzing the three-dimensional SPM images with the image analyzer, and the result was

Table II The Morphological Patterns of Samples Prepared, and the Notation

Content of T-12 (wt/wt %)	Content of BPO (wt/wt %)	Morphological Pattern	Sample Notation
0.025	1.0	Sea-island	SI-1
0.050	1.0	Sea-island	SI-2
0.050	3.0	Sea-island/Cocontinuous	SI/CC
0.050	5.0	Cocontinuous	CC

shown in Figure 6. For the samples with sea-island morphology, the roughness was decreased, as the content of T-12 was increased, because the viscosity of the reacting mixture was increased and the phase separation was suppressed. The roughness of CC was lower than SI-1 and SI/CC, because the polymerization rate of styrene was increased with increasing the BPO content and gelation of the PS, after which the phase separation was stopped, which occurred earlier. SI-2 had a smoother surface than other samples, because the viscosity during the phase separation

was very high, and the growth of the separated nuclei was restricted.

Swelling Behavior in Water

Figure 7 shows the swelling behavior with water. Generally, it has been known that the swelling behavior of the polymer blend is strongly influenced by its heterophase structure. When the IPNs of hydrophilic and hydrophobic components are swollen in water, the water diffuses through the hydrophilic phase. At a fixed composition, the swelling ratio in water decreases as the degree of intermixing increases. In Figure 7, the equilibrium swelling ratio of PU/PS IPN having the sea-island morphology was higher, compared to the samples with cocontinuous morphology. If the hydrophilic PU-rich phase formed the matrix and the hydrophobic PS phase formed the dispersion, the swelling of the matrix in water was not restricted. But if the hydrophobic PS phase also formed a continuous phase, the swelling of the hydrophilic PU phase was restricted by the neighboring hydrophobic PS phase. The swelling behavior also reflected the morphology difference of SI, SI/CC, and CC.

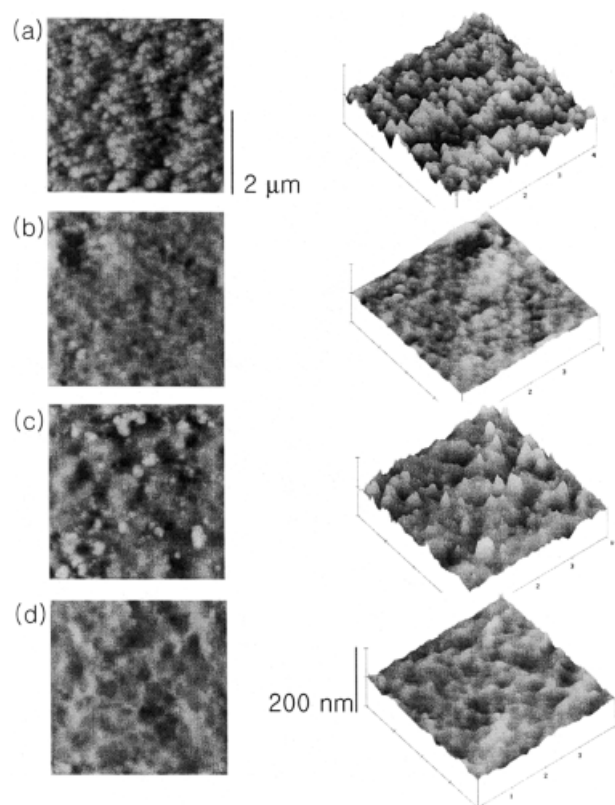


Figure 5 SPM images of surface morphology of PU/PS IPNs: (a) SI-1; (b) SI-2; (c) SI/CC; (d) CC.

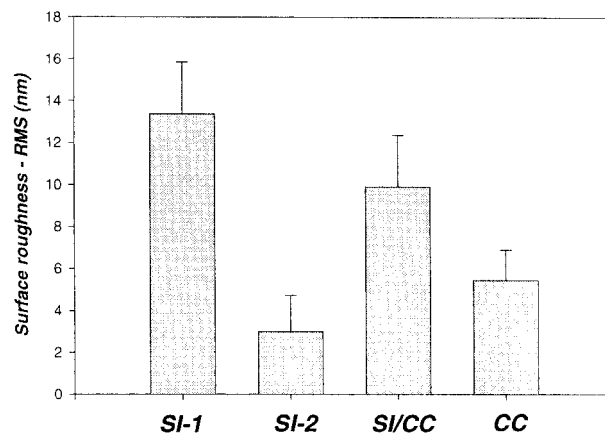


Figure 6 Surface roughness of PU/PS IPNs.

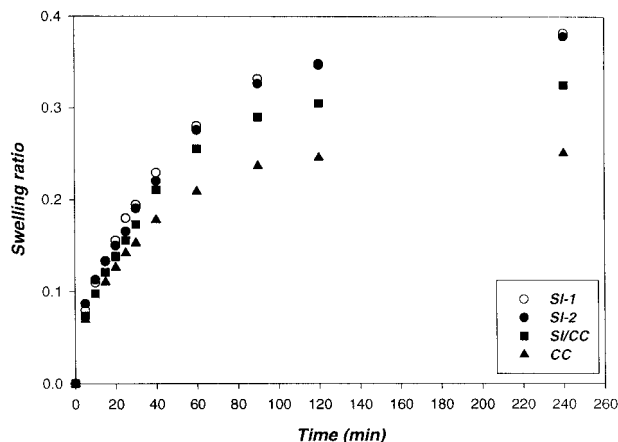


Figure 7 Swelling behavior with water of PU/PS IPNs.

Interfacial Energy

Figure 8 shows the interfacial energy with water. The result of interfacial energy measurement showed a similar trend with swelling behavior with water. Interfacial energy between water and PU/PS IPN having sea-island morphology was lower than the sample with cocontinuous morphology, which means that the surface became more hydrophilic, with the swollen and expanded PU phase on the surface.

Fibrinogen Adsorption

Fibrinogen is one of the most important globular proteins circulating in the blood. It plays a central role in the regulation of hemostasis and thrombosis by participating in blood coagulation and facilitating adhesion and aggregation of platelets. Fibrinogen is a relatively large (340 kDa) glycoprotein composed of two each of three nonidentical polypeptide chains ($A\alpha_2B\beta_2\gamma_2$). The molecule is folded in such a way that all six amino termini are clustered in a central domain (E domain), but the three different carboxyl ends are located at opposite ends of distended molecule (D domain), which are connected to the central domain by three-stranded "coiled coils." These D domains can be split and displaced from the molecular axis, and each coiled-coil rod was interrupted by a small globular region to form an added globular region adjacent to the central E domain through the folding of $A\alpha$ chains. This macromolecular dimensions and conformation of hydrated fibrinogen considerably affects surface-dependant interaction.^{23–25} Generally, proteins are heterogeneous molecules and contain regions of differing

polarity, charge, and hydrophilicity. Thus, proteins exhibit amphoteric, and amphiphilic properties, and the net structure is a spontaneously folding pattern with hydrophobic core and complex irregular exterior surface formed by the polar or hydrophilic side chains. Adsorption to the surface may invoke the breakage of amphiphilic balance and conformational changes in the protein, and cause the proteins to denature.^{12,26} In this test, BPF was adsorbed rapidly within a few minutes, and then reached equilibrium. Relatively large amounts of BPFs were adsorbed on the SI-1 compared with other samples (Fig. 9). Dimer, trimer, and macromer of the hydrated fibrinogen have linear conformations predominantly, and increased affinity for the hydrophobic surface compared with monomeric fibrinogen.²⁴ However, the sample surfaces in this study showed similar value of interfacial energy with water, that is, similar hydrophilicity. Otherwise, the difference of surface roughness was large enough to affect the conformational change of fibrinogens adsorbed, and adsorption kinetic of fibrinogen. Thus, it became a predominant factor on the adsorption of fibrinogens, and the formation of adsorbed multiplayer of fibrinogens.^{9–13,27} SI-1 had a rougher surface than the other samples, and relatively large amounts of BPFs were adsorbed upon the SI-1 compared with the other samples. However, SI-2, and CC had relatively smooth surfaces compared with the surface of SI-1, and the adsorption of BPFs was suppressed.

Platelet Adhesion

The interaction of platelets with the surfaces of PU/PS IPNs was investigated by using PRP pre-

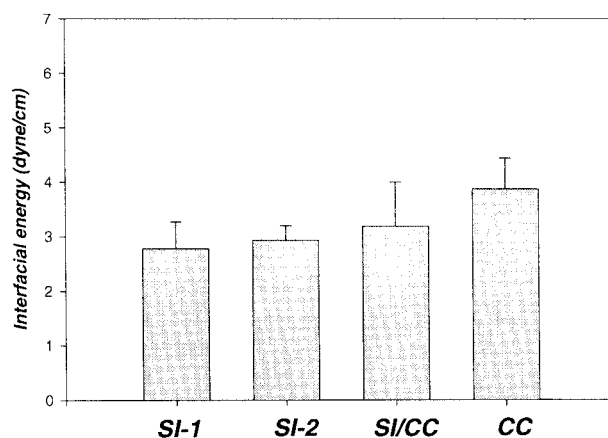


Figure 8 Interfacial energy between PU/PS IPNs and water.

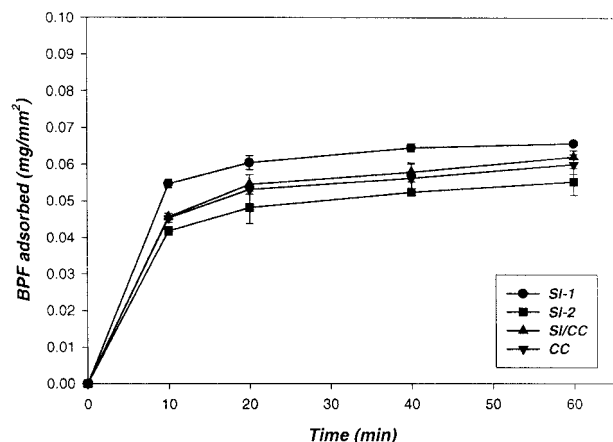


Figure 9 Amount of fibrinogens adsorbed on PU/PS IPNs.

pared from human whole blood. Unstimulated platelets shows a 2- μm discoid shape, and functioning platelets are divided into three zones: the peripheral, sol-gel, and organelle.²⁸ The peripheral zone consists of the platelet membrane, the open canalicular system, and the exterior coat of the platelet (rich in glycoproteins). Platelet glycoproteins form the basis of the platelet receptor system for activation, and the sol-gel zone contains a fibrillar contractile system that allows

shape change, pseudopod formation, and contraction. In the platelet adhesion test, platelets initially react with the surface by pseudopod formation, and then form aggregates through the binding of glycoproteins. In the BPF adsorption test, the surface roughness was a predominant factor on the adsorption. As a result, relatively large amounts of BPFs were adsorbed on SI-1, having the roughest surface among PU/PS IPN samples. The platelets are easy to adhere to the surface where a large amount of fibrinogens are previously adsorbed, because the preadsorbed fibrinogens cause excessive assembly of the glycoproteins on the platelets. In Figure 10, a large amount of platelets were adhered to the surface of SI-1 compared with other surfaces. However, the platelets adhesion was suppressed to SI-2 and CC surfaces, that is, relatively smooth surfaces.

CONCLUSIONS

In this study, we controlled the reaction rate, gelation time, rate of phase separation, and phase separation time during the synthesis of hydrophilic PU/hydrophobic PS IPNs. As a result, two samples (SI-1, SI-2) with sea-island morphology, of which the size of PS-rich domain was different

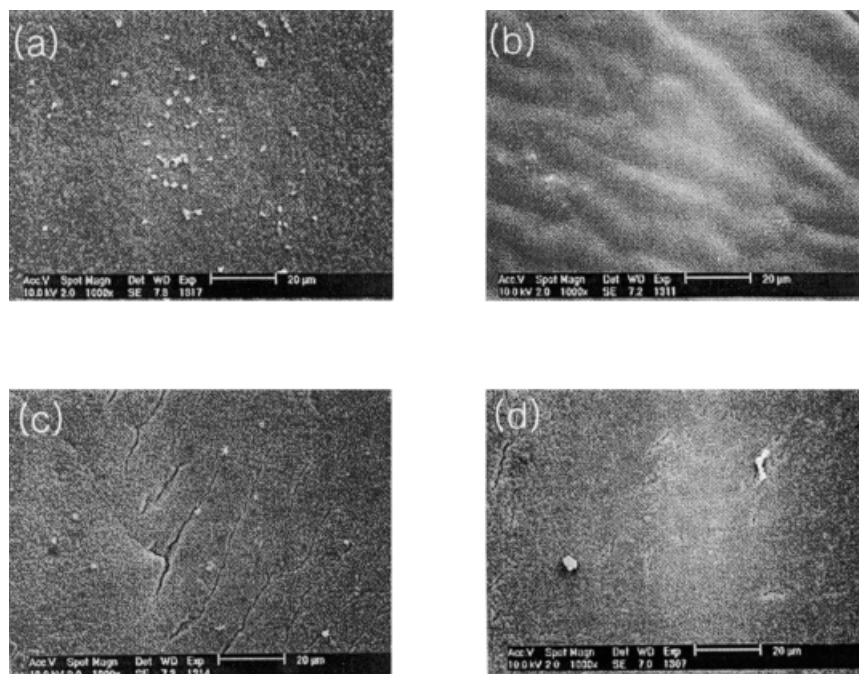


Figure 10 SEM photographs of adhered platelets on PU/PS IPNs: (a) SI-1; (b) SI-2; (c) SI/CC; (d) CC.

from each other, were obtained, when the polymerization rate of PS was relatively slow and the phase separation time was long. SI-2 had smaller PS-rich domains, and a smoother surface, compared to SI-1, because viscosity at the onset of phase separation was higher. When the polymerization rate of PS was relatively fast, and phase separation time was short, a relatively smooth sample (CC) with cocontinuous morphology was obtained, and when the polymerization rate of PS was relatively intermediate, a sample (SI/CC) with dual phase morphology was also obtained. The CC surface was smoother than SI/CC, because the gelation of PS occurred earlier, and the phase separation was stopped.

The swelling ratio with water increased, and interfacial energy with water decreased, as the phase continuity decreased, which indicated that the surface became more hydrophilic with swollen and expanded hydrophilic PU.

The blood-compatibility tests showed that the surface roughness was a very important factor on the adsorption of fibrinogens and platelets in this study. A large amount of fibrinogen, and platelets were adsorbed on the relatively rough surface of SI-1 compared with SI-2, and CC with smooth surfaces.

This study showed that the degree of phase separation, surface hydrophilicity, and specially surface roughness, which highly affect the non-thrombogenic character of surface, could be changed by controlling the morphology, and the results may be very useful in the designing of blood-contacting biomedical polymers.

REFERENCES

1. Olabisi, O.; Robeson, L. M.; Shaw, M. T. *Polymer-Polymer Miscibility*; Academic Press: New York, 1979.
2. Paul, D. R.; Newman, S. *Polymer Blends*; Academic Press: New York, 1978.
3. Utracki, L. A. *Polymer Alloys and Blends*; Oxford University Press: New York, 1989.
4. Klempner, D.; Sperling, L. H.; Utracki, L. H., Eds. *Interpenetrating Polymer Networks*; Adv. Chem. Ser. No. 239; ACS Books: Washington, DC, 1994.
5. Sperling, L. H. *Interpenetrating Polymer Networks and Related Materials*; Plenum: New York, 1981.
6. Klempner, D.; Frisch, K. C., Eds. *Advances in Interpenetrating Polymer Networks*; Technomic: Lancaster, PA, 1994, Vol. IV.
7. Kim, S. C.; Sperling, L. H. *IPNs Around the World*; Science and Engineering: John Wiley & Sons. Inc.: New York, 1997.
8. Mishra, V.; Du Prez, F. E.; Gosen, E.; Goethals, E. J.; Sperling, L. H. *J Appl Polym Sci* 1995, 58, 331.
9. Lampin, M.; Clerout, R. W.; Legris, C.; Degrange, M.; Sigot-Luizard, M. F. *J Biomed Mater Res* 1997, 36, 99.
10. Kanagaraja, S.; Alaeddine, S.; Eriksson, C.; Lausmaa, J., et. al. *J Biomed Mater Res* 1999, 46, 582.
11. Onda, M.; Lvov, Y.; Ariga, K.; Kuntake, T. *Jpn J Appl Phys* 1997, 36, 1608.
12. Lamba, N. M. K.; Woodhouse, K. A.; Cooper, S. L. *Polyurethanes in Biomedical Applications*; CRC Press: Boca Raton, FL, 1998.
13. You, H. X.; Lowe, C. R. *J Colloids Interface Sci* 1996, 182, 586.
14. Shin, Y. C.; Han, D. K.; Kim, Y. H.; Kim, S. C. *J Biomater Sci Polym Ed* 1994, 6, 195.
15. Shin, Y. C.; Han, D. K.; Kim, Y. H.; Kim, S. C. *J Biomater Sci Polym Ed* 1994, 6, 281.
16. Roh, H. W.; Song, M. J.; Han, D. K.; Lee, D. S.; Ahn, J. H.; Kim, S. C. *J Biomater Sci Polym Ed* 1999, 10, 123.
17. Kim, J. H.; Song, M. H.; Roh, H. W.; Shin, Y. C.; Kim, S. C. *J Biomater Sci Polym Ed* 2000, 11, 197.
18. Perrin, D. D.; Armarego, W. L. F.; Perrin, D. R. *Purification of Laboratory Chemicals*; Pergamon Press: New York, 1980, 2nd ed.
19. David, D. J.; Staley, H. B. *Analytical Chemistry of the Polyurethanes*; Wiley-Interscience: New York, 1969.
20. Andrade, J. D.; Ma, S. M.; King, R. N.; Gregonis, D. E. *J Colloid Interface Sci* 1979, 72, 488.
21. Ishihara, K.; Fujiike, A.; Iwasaki, Y.; Kurita, K.; Nakabayashi, N. *J Polym Sci Part A Polym Chem* 1996, 34, 199.
22. Han, D. K.; Jeong, S. Y.; Kim, Y. H. *J Biomed Mater Res Appl Biomater* 1989, 23, 211.
23. Feng, L.; Andrade, J. D. In *Hobett, T.; Brash, J., Eds.; Proteins at Interfaces—II*; American Chemical Society Symposium: Washington, DC, 1995.
24. Marchant, R. E.; Barb, N. D.; Shainoff, J. R.; Eppell, S. J.; Wilson, D. L.; Siedlecki, C. A. *Thromb Haemost* 1997, 77, 1048.
25. Everse, S. J.; Spraggon, G.; Doolittle, R. F. *Thromb Haemost* 1998, 80, 1.
26. Ratner, B. D.; Hoffman, A. S.; Schoen, F. J.; Lemons, J. E. *Biomaterials Science*; Academic Press Inc.: New York, 1996.
27. Tsuruta, T.; Hayashi, T.; Kataoka, K.; Ishihara, K.; Kimura, Y. *Biomedical Applications of Polymeric Materials*; CRC Press Inc.: Boca Raton, FL, 1996.
28. Body, S. C. *J Cardiovasc Pharmacol* 1996, 27, S13.